

# Development of high precision Coordinate Measuring Machine - Uncertainty analysis of multi-probe method -

Tomohiko Takamura<sup>1,#</sup>, Ping Yang<sup>1</sup>, Satoru Takahashi<sup>1</sup>, Kiyoshi Takamasu<sup>1</sup>,  
Osamu Sato<sup>2</sup>, Sonko Osawa<sup>2</sup> and Toshiyuki Takatsuji<sup>2</sup>

<sup>1</sup> Department of Precision Engineering, The University of Tokyo, Tokyo 113-8656, Japan

<sup>2</sup> National Institute of Advanced Industrial Science and Technology (AIST), Ibaraki 305-8563, Japan

# Corresponding author / takamura@nanolab.t.u-tokyo.ac.jp, TEL: +81-3-5841-6472

KEYWORDS : CMM, multi-probe method, laser interferometer, autocollimator, kinematic error

With the development of micro system technology, the demands for three-dimensional (3D) metrology in the mesoscopic range have been increased. To satisfy these requirements, A high precision Micro-CMM called M-CMM targeting 50nm uncertainty is under development. In order to improve the motion accuracy of each stage on the Micro-CMM, a multi-probe measurement system has been designed and established. The multi-probe scanning system is composed of three laser interferometers and one autocollimator. The autocollimator measures the yaw error of the moving stage, while three laser interferometers simultaneously probe the surface of a reference bar mirror which is fixed on top of the moving stage. The straightness motion error and the reference bar mirror profile are reconstructed by an application of simultaneous equation and least-squares methods.

From the experiment results, we conclude that the systematic error can't be ignored. We evaluate systematic error of nonlinear parameters such as the alignment errors and accuracy of the moving stage. To verify the systematic error, we add non linear parameter to the simulation program. The simulation result shows that yaw error affects systematic error, while random error consists mainly of laser interferometers' error.

Manuscript received: January XX, 2011 / Accepted: January XX, 2011

## NOMENCLATURE

$\mathbf{Y}$  = measuring vector

$\mathbf{A}$  = jacobian matrix

$\mathbf{X}$  = parameter vector

$\mathbf{S}$  = weight matrix

$m_k(x)$  = the kth laser interferometer's output at  $x$

$m_a(x)$  = the autocollimator's output at  $x$

$f(x)$  = the profile of the bar mirror at  $x$

$e_s(x)$  = the straightness error of the moving stage at  $x$

$e_y(x)$  = the yaw error of the moving stage at  $x$

$u$  = the sensor offset constant

## 1. Introduction

### 1.1 Research background

As part of the trend toward miniaturization and modularization in microsystem technology, the requirements of measuring nano- and microstructures with 3D measurement uncertainty within the range of 0.1  $\mu\text{m}$  have increased. However, conventional measuring methods cannot satisfy the requirements, because the measurement scales of conventional coordinate measuring machines (CMMs) are usually several tens of millimeters or more, which is not suitable for measuring small parts of submillimeter or even submicrometer order. In addition, the conventional CMMs lack the level of 3D measurement uncertainty and are not supplied with the proper probing systems in many applications [1]. Therefore, micro-CMMs with special micro-probe systems for 3D metrology

with high-aspect-ratio micro parts are currently being developed to satisfy the described requirements. Some of the micro-CMMs are discussed, and their specifications are shown in Table 1.

A novel high-precision micro-CMM called M-CMM has been developed, and a prototype has been built at the Advanced Industrial Science and Technology (AIST). We are aiming at a measurement uncertainty of 3D-coordinates of about 50 nm. To develop the motion accuracy of each stage of the M-CMM, we propose a multi-probe method and discuss its use for evaluating yaw and straightness motion errors.

Micro-CMMs	Range-XYZ[mm]	Uncertainty[nm]
Isara <sup>[2]</sup>	100×100×40	30
F25	100×100×100	Less than 100
M-NanoCoord <sup>[3]</sup>	200×200×100	200
M-CMM	160×160×100	Aim for 50

Table 1 Specification comparisons of micro-CMMs

### 1.2 Configuration of the M-CMM

The configuration of the M-CMM includes three main parts, the Z-axis, probe unit, and XY stage. Each axis has a linear motion stage system composed of air-bearing sliders, glass linear scale, moving table, driving motor and related parts. The linear motion stage systems have been applied successfully to precision measurement systems because the air bearings have no friction and the area averaging effect on the guide error provides high positioning accuracy and low traveling motion error. In addition, the linear scales feedback the position signal within the range of nanometer resolution.

There are three special specifications in the design of the M-CMM. First, the main structure of each axis is made of alumina ceramic that has high rigidity and a low coefficient of thermal expansion (CTE = 5.3 ppm/K), and the base plate of the M-CMM is made of granite of 5 ppm/K CTE. Therefore, the M-CMM has good performance in response to temperature changes, and the thermal deformation due to the driving heat and temperature changes can be significantly reduced.

Second, we divided the XYZ axis into two mechanical parts. One is the Z-axis, which was separately designed and built. The other is the XY-axis, which was stacked in two linear stages. The reason is that the sensitivity of the 3D contacting micro-probes in the Z-direction is usually lower than that in the XY plane because probing direction the length of the stylus has an effect in the horizontal. Therefore, the measurement uncertainty of the Z-axis is larger than that of XY-axis.

Third, the probe unit has a changeable connector by which the M-CMM can use different kinds of contacting probe systems and do the measurement with different levels of uncertainty.

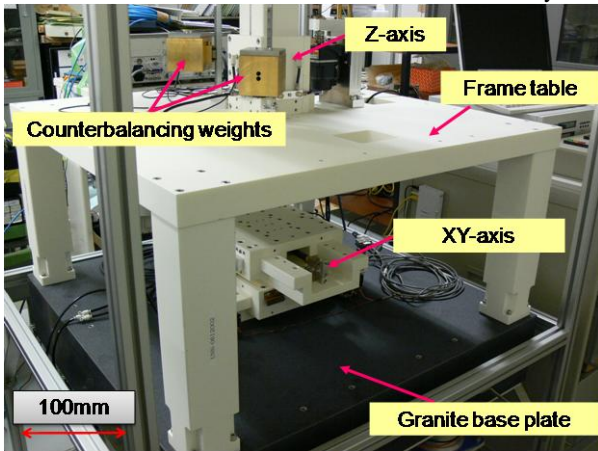


Fig. 1 Main Structure of M-CMM

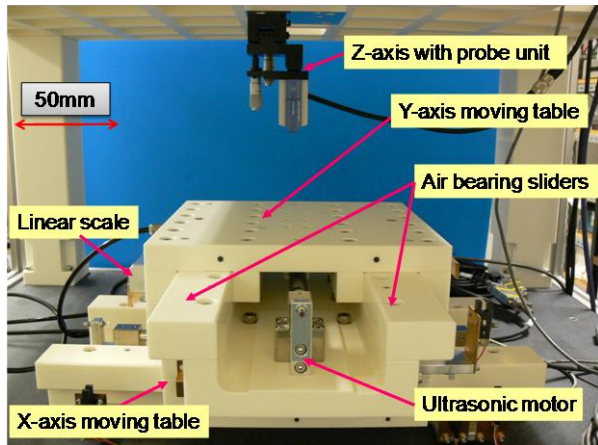


Fig. 2 Structure of XY stage and probe unit

**2 Calibration of the M-CMM**

**2.1 DOF and Abbe error on the M-CMM**

In a three-dimensional space, any positioning stage is considered to have six degrees of freedom (DOF): three translational errors and three rotational errors. Abbe errors are caused by the rotational errors of relative translations between the measurement object and probe device, and the offset between the reference and the measurement point. Often Abbe errors are the most important uncertainty sources in dimensional metrology applications aiming for measurement uncertainties of only a few nanometers [4]. For example, the Abbe error  $\delta$  is approximately 10 nm of error based on a 10 mm moment arm  $H$  and a tilt of  $1 \mu\text{rad}$   $\theta$  (Fig. 4). Therefore, the 6DOF of each stage on M-CMM is a very i

important factor in the development of high-precision micro-CMMs.

The motion accuracy values of the M-CMM without any compensation are shown in Table 3. For instance, the value of the Abbe error of the XY-axis can be in the range of micrometers. So the motion errors of the XY stage on the M-CMM should be measured and calibrated. The traditional calibration method using only a single sensor is up to the high accuracy of the reference mirror, because the motion errors are also present. To take this into account, an error separation technique employing several displacement probes was proposed and developed, and other applications using the multi-probe have been widely used in precision measurement [5, 6]. In our measurement system, we use the multi-probe method to measure the yaw and straightness motion errors of each linear stage, and the profile of a standard mirror is also reconstructed by application of the simultaneous equation and least-squares methods [7-9].

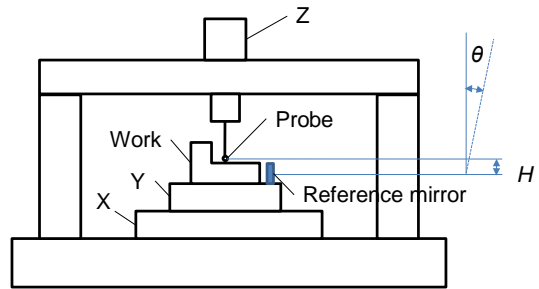


Fig. 3 Illustration of an Abbe error after compensation

Axis	Degree of freedom	Accuracy / range
X,Y	Straightness	Max: 0.5 $\mu\text{m}$ / 160mm
X,Y	Tilting	Max: 8 $\mu\text{rad}$ / 160 mm
Z	Straightness	Max: 0.3 $\mu\text{m}$ / 100 mm
Z	Tilting	Max: 5 $\mu\text{rad}$ / 100 mm

Table 3 Motion accuracy of M-CMM without compensation

**2.2 The principle of the multi-probe method**

In the measurement system, one autocollimator measures the yaw error of the stage, and multiple laser interferometers measure the profile of a bar mirror fixed on the top of the XY-axis. Unlike fixing the position sensors on a moving scanner, the laser interferometers are mounted stationary, as shown in Fig. 5 [15,16].

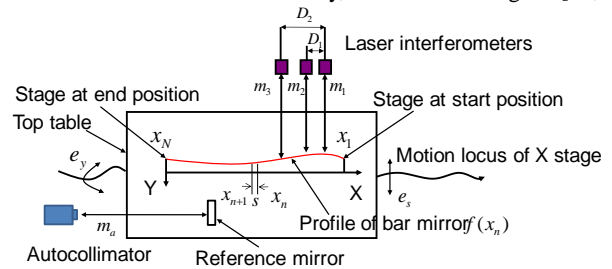


Fig. 4 Principle of the multi-probe method

When let the corresponding laser interferometers and autocollimator outputs be  $m_i(x_n)$  and  $m_a(x_n)$ , the three probes system outputs can be expressed as follows:

$$\begin{aligned}
 m_1(x_n) &= f(x_n + 0) + e_s(x_n) + 0 \cdot e_y(x_n) + u_1 \\
 m_2(x_n) &= f(x_n + D_1) + e_s(x_n) + D_1 \cdot e_y(x_n) + u_2 \\
 m_3(x_n) &= f(x_n + D_2) + e_s(x_n) + D_2 \cdot e_y(x_n) + u_3 \\
 m_a(x_n) &= e_y(x_n) + u_a \\
 n &= 1 \dots N_s
 \end{aligned}
 \tag{1}$$

where  $f(x_n)$  denotes the profile of the bar mirror, and  $e_y(x_n)$  and  $e_s(x_n)$  are the yaw and straightness motion errors of the moving stage.  $D_1$  is the interval of the 2nd to the 1st laser interferometer, and  $D_2$  is the interval of the 2th to the 1st laser interferometer.  $N_s = N - D_2$  is the numbers of sampling points and  $N$  is

the sampling point of the bar mirror when  $s = 1$  is the measuring step distance of sampling points.  $u$  are the offsets of each probe.

Eq. (1) can be compactly written with matrix style expressions as follows:

$$\mathbf{Y} = [m_1(x_{1...N_s}), m_2(x_{1...N_s}), m_3(x_{1...N_s}), m_4(x_{1...N_s})]^T$$

$$\mathbf{X} = [f(x_{1...N-2}), e_s(x_{1...N_s}), e_y(x_{1...N_s}), c_1, c_2]^T \quad (2)$$

$$\mathbf{A} = \frac{\partial \mathbf{Y}}{\partial \mathbf{X}}$$

$$\mathbf{Y} = \mathbf{A}\mathbf{X}$$

where  $\mathbf{Y}$  and  $\mathbf{X}$  denote the measuring vector and parameter vector or involving the profile of bar mirror and the motion errors, respectively. The jacobian matrix  $\mathbf{A}$  is calculated from  $\mathbf{Y}$  and  $\mathbf{X}$ . The offset constants  $c_1$  and  $c_2$  are differences of  $u$ .

In the analysis, the parameters are reconstructed by the weighted least-squares methods using pseudo inverse matrix as follows:

$$\mathbf{S} = \text{diag}(\sigma_{m_1}^2(x_{1...N_s}), \sigma_{m_2}^2(x_{1...N_s}), \sigma_{m_3}^2(x_{1...N_s}), \sigma_{m_4}^2(x_{1...N_s})) \quad (3)$$

$$\mathbf{X} = (\mathbf{A}^T \mathbf{S}^{-1} \mathbf{A})^{-1} \mathbf{A}^T \mathbf{S}^{-1} \mathbf{Y}$$

This means that multi-probe method calculate the each parameters; the kinematic errors and the mirror profile, independently. The diagonal matrix  $\mathbf{S}$  denotes the uncertainty of laser interferometers and autocollimator. The condition of solution existing is  $\text{GC D}(D_1, D_2) = s$ , and  $s$  may be smaller than the physical interval of probes.

### 3. Pre-experiment of the three point method

#### 3.1 Configuration of the pre-experiment

The pre-experiment of the multi-probe method is designed to measure the motion accuracy of an XY stage based on a stepper motor system. In the pre-experiment, one autocollimator measures the yaw error of the stage and three laser interferometers measure the profile of a standard mirror fixed on the top of the XY stage. Fig. 5 shows the main setup of the pre-experiment, which is composed of optical reflection devices, an XY stepper motor stage, laser interferometers, receivers, beam splitters, optical reflection mirrors, and an autocollimator. The optical reflection devices that are fixed on the top of the XY stage consist of a bar mirror, a housing for the bar mirror, and a reference mirror (mirror 6). (Fig. 6)

The pre-experiment was measured by three laser interferometers and one autocollimator at the same time. The laser interferometers probed the profile of the bar mirror and the autocollimator measured the yaw error of the XY stage by the reference mirror 4 (Fig. 10). The valid size of the bar mirror was about 100 mm×30 mm with an accuracy of  $\lambda = 632.8$  nm. The sampling length of the bar mirror was 101 mm. When the intervals of laser interferometers are  $D_1 = 10$  mm and  $D_2 = 11$  mm, the sampling interval is  $s = 1$  mm which is smaller than  $D$ . The number of sampling points on the bar mirror  $N$  is 101, and the number of sampling points on the stage  $N_s$  is 80.

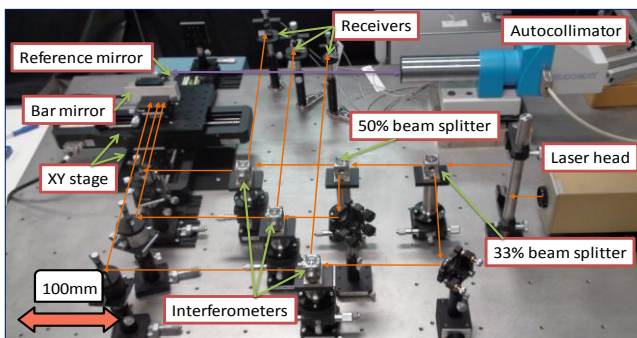


Fig. 5 Main set up of the pre-experiment

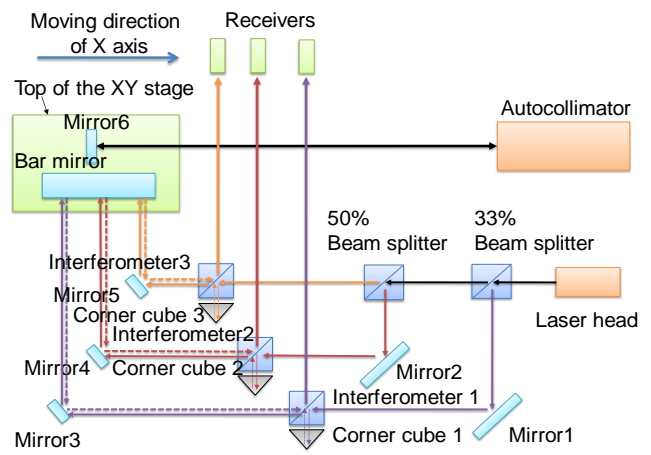


Fig. 6 Block chart of the pre-experiment

#### 3.2 Results of the pre-experiment

During ten repetitions of the experiment, the yaw errors of the X-axis are presented in Fig. 7. The range of the yaw error is about 20  $\mu\text{rad}$ . According to the application of the simultaneous equation and least-squares methods, the straightness errors of the X-axis are showed in Fig. 8. The range of the straightness motion error is about  $\pm 1 \mu\text{m}$ . The reconstructed profiles of the bar mirror are shown in Fig. 9, and the repeatability is good. If we consider standard deviation of each sensor as  $\sigma_{m1} = \sigma_{m2} = \sigma_{m3} = 8$  nm, and  $\sigma_{ma} = 0.4 \mu\text{rad}$ , the uncertainty of the multi-probe method in the pre-experiment ( $\pm 2\sigma$ ) is 9 nm, as shown in Fig. 10, and the profile standard deviation of the bar mirror calculated from the pre-experiment is compared with the theoretical uncertainty of the multi-probe method. The Fig. 10 shows that the standard deviation of the bar mirror profile is mainly in the range of  $\pm 2\sigma$ . The multi-probe method performs well in the real application.

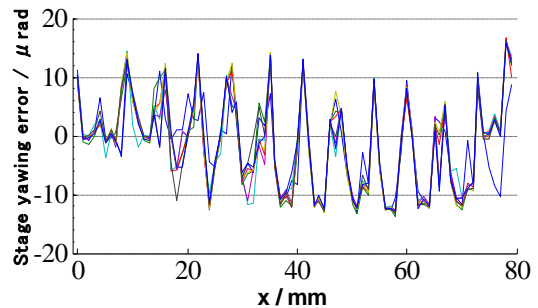


Fig. 7 Yaw error of moving stage

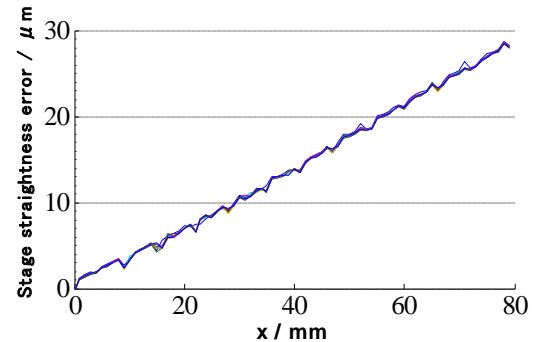


Fig. 8 Straightness error of moving stage

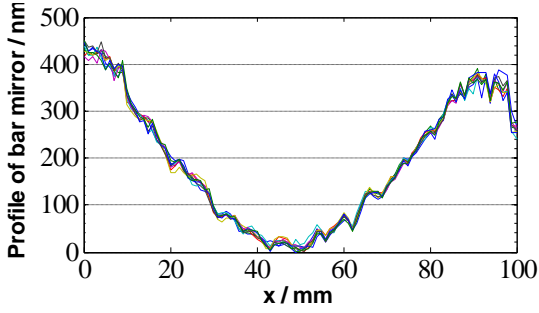


Fig. 9 Profile of bar mirror

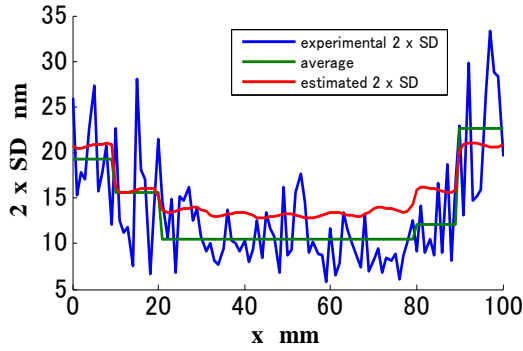


Fig. 10 Experimental and estimated uncertainty

#### 4. Evaluation of the pre-experiment

##### 4.1 Comparisons to the whitelight interferometer

To validate the results of the pre-experiment, we compared the results with that of the white light interferometer. The result of the pre-experiment is mean of 10 times measurement results. The results of the white light interferometer measurement are done by zygo's one before and after the pre-experiment. Because a result of the white light interferometer measurement is generally filtered, we applied the 5 points moving average filter to the results of pre-experiment too to compare.

As the white light interferometer measures the plain profile, we sliced the proper line profile to compare shown in Fig. 11 The result of comparisons is shown in Fig. 12 We conclude that they are equal because the doubled standard deviation of flat area; 9 nm is smaller than 10 nm.

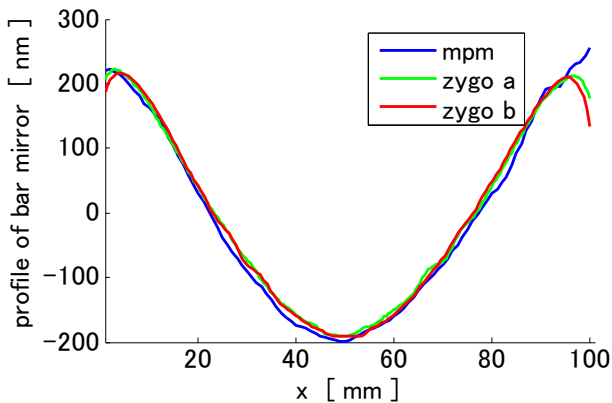


Fig. 11 The mirror profile of each measurement

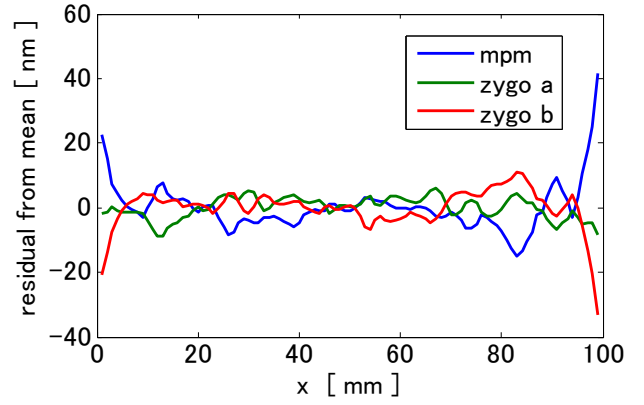


Fig. 12 Comparisons of the mirror profile

##### 4.2 The difference between filtered and non filtered

While the filtered results of the pre-experiment correspond to that of the white light interferometer measurement, the non filtered results don't correspond. So we evaluate the effect of averaging filter on the condition that filtered result is enough precise. The difference between the mirror profile with MA filter and with no filter is shown in Fig. 13. Their uncertainty is 25 nm and show the repeatability while the measurement uncertainty is 11 nm. This means that the systematic error can't be ignored.

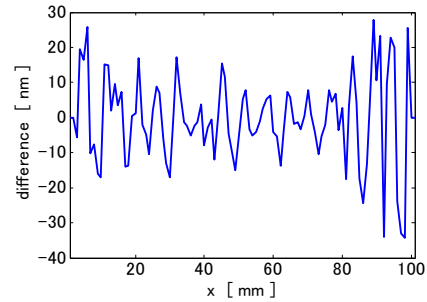


Fig. 13 Differences between filtered and non filtered

#### 5. Estimation of the systematic errors

##### 5.1 The change of the measuring vector

Because the systematic error can't be ignored, we estimated the effect of the systematic errors. At first, we discuss about the change of the measuring vector with non linear term. The non linear measuring vector can be expressed as follows:

$$m_k^{nl}(x_n) = f(x_n + D_k + \delta x_k(x_n)) + \delta x_k(x_n) \cdot e_y(x_n) + opd_k(\theta) + e_s(x_n) + u_k + D_k \cdot e_y(x_n) \quad (4)$$

$$m_a(x_n) = e_y(x_n) + u_a$$

where  $\delta x_k$  is positioning uncertainty of the kth probe and  $opd_k$  is the optical path difference of the kth probe.

As shown in Fig. 14 (a),  $\delta x_k$  can be expressed as follows:

$$\delta x_k(x_n) = eD_k + e_x(x_n) + D_k \left( \frac{1}{\cos(e_y(x_n))} - 1 \right) \quad (5)$$

where  $eD_k$  is the alignment error of the kth probe,  $e_x$  is moving stage's x positioning error and last term is probe interval changing from yaw error. We estimate that the standard deviation of  $eD_k$  is 100  $\mu\text{m}$  as we align the probes with CCD, that of  $e_x$  is 20  $\mu\text{m}$  from the moving stage's specification and last term is less than 1 nm from the result of pre-experiment. The total standard deviation of  $\delta x_k$  is 120  $\mu\text{m}$ .

This positioning uncertainty affects to measuring vector. When we assume that  $e_y = 10\mu\text{rad}$  and  $f = 5 \text{ nm}$ , the difference caused by  $\delta x_k$  can be expressed as follows.

$$\delta x_k(x_n) \cdot e_y(x_n) \approx 1 \text{ nm}$$

$$f(x_n + D_k + \delta x_k(x_n)) = f'(x_n + D_k) \cdot \delta x_k(x_n) \approx 2 \text{ nm}$$

As shown in Fig. 14 (b),  $opd_k$  can be expressed as follows:

$$\begin{aligned} opd_k(\vartheta) &= 2opl_k \cdot (\sec(\vartheta) - 1) = opl_k \cdot \vartheta^2 + o(\vartheta^4) \\ \vartheta^2 &= (e_{yaw} + \varphi_{align})^2 \\ &= \varphi_{align}^2 + 2\varphi_{align}e_{yaw} + e_{yaw}^2 \\ &= 2\varphi_{align}e_{yaw} + o(10^{-10}) + const \end{aligned} \quad (6)$$

where  $opl_k$  is the optical path length of the  $k$ th probe which are 500 mm and  $\theta$  is the angle between the optical path coordinate and the moving stage coordinate which consists with the moving stage's angle alignment error and the yaw error. We estimate that the angle alignment error is 500  $\mu$ rad from the result of pre-experiment.

This optical path difference also affects to measuring vector. Because constant value stands for the trans offset, the difference caused by  $opd_k$  can be expressed as follows.

$$\begin{aligned} opd_k(e_{yaw}) &= 2opl_k \varphi_{align} e_{yaw} \\ opd(e_{yaw}) &\approx 2 \times 0.5 \times 500 \times 10^{-6} \times 10 \times 10^{-6} = 5 \text{ nm} \end{aligned}$$

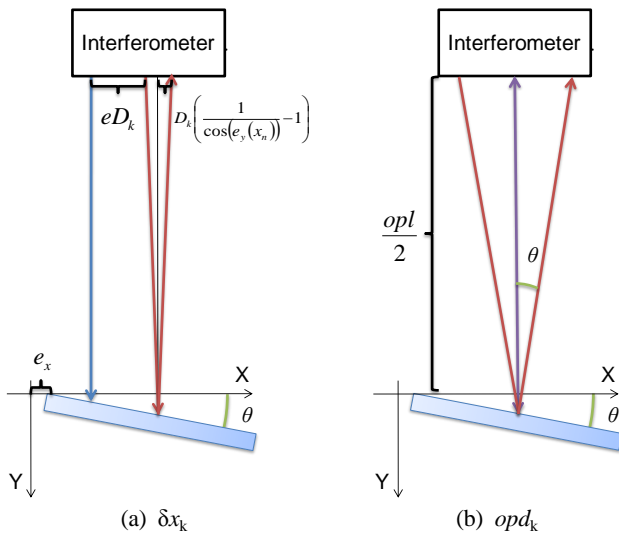


Fig. 14 The effect of non linear terms

## 5.2 The change of the jacobian matrix

Secondly, we discuss about the change of the jacobian matrix with non linear terms. When we apply the Eq. (4), we should also apply the following equations:

$$\begin{aligned} \mathbf{A}^{nl} &= \frac{\partial \mathbf{Y}^{nl}}{\partial \mathbf{X}} \\ &= \frac{\partial}{\partial \mathbf{X}} \left( [m_1^{nl}(x_i), m_2^{nl}(x_i), m_3^{nl}(x_i), m_a(x_i)] \right) \end{aligned} \quad (7)$$

$$\mathbf{X}^{nl} = (\mathbf{A}^{nlT} \mathbf{S}^{-1} \mathbf{A}^{nl})^{-1} \mathbf{A}^{nlT} \mathbf{S}^{-1} \mathbf{Y}^{nl}$$

But we cannot solve analytically, because these equations are non linear polynomials. In the following simulations, we assume non linear parameters in the jacobian matrix as constant. This method cannot apply to the real measurement, but is enough for evaluate the effect of the change of the jacobian matrix as its a ct as linear polynomials.

## 6. Simulation with non linear parameters

### 6.1 The parameters of simulation

To evaluate the effect of non linear parameters, we performed some simulations. Because the purpose of the simulation is to reproduce the systematic error of the pre-experiment, most parameters are same to the pre-experiment's one. The bar mirror profile is a convex sine curve whose height is 400 nm (Fig. 15) and the yaw error and the straightness error of the moving stage is mean of the results of the pre-experiment (Fig. 16).

Since the yaw error affects to the non linear terms, we define the uncertainty of the autocollimator as  $\sigma_{ma} = 0.5 \mu$ rad, besides

the uncertainty of the laser interferometers as  $\sigma_{mk} = 0.01 \text{ nm}$  to fasten the consequence and not to make rankkkk. The sampling length of the bar mirror is 101 mm, the intervals of laser interferometers are  $D_1 = 10 \text{ mm}$  and  $D_2 = 11 \text{ mm}$ , the sampling interval is  $s = 1 \text{ mm}$ , the number of sampling points on the bar mirror  $N$  is 101 and the number of sampling points on the stage  $N_s$  is 80.

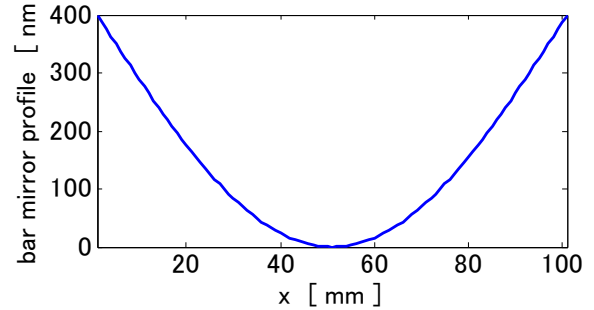


Fig. 15 Profile of bar mirror

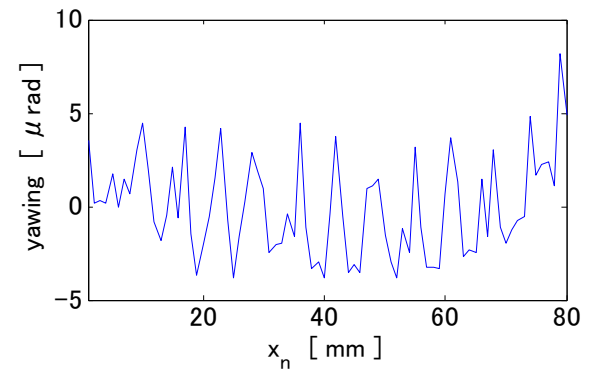


Fig. 16 Yaw error of moving stage

### 6.2 Effect of the measuring vector

We performed the simulations to evaluate the effect of the measuring vector difference. At first, we constructed the  $\mathbf{Y}^{nl}$  from the parameters. Then we reconstructed the  $\mathbf{X}^{nl}$  from  $\mathbf{A}$  and  $\mathbf{Y}^{nl}$ . At last, we compared the 1000 times results mean of the reconstructed  $\mathbf{X}^{nl}$  with the original  $\mathbf{X}$ . The non linear parameters are defined as followed:

- Only the positioning uncertainty  $\delta x_k$ 
  - $eD_k$  : 100 mm
  - $e_x$  : 20 mm
  - $\varphi_{align}$  : 0 mrad
  - $opl_k$  : 0 mm
- Only the optical path difference  $opd_k$ 
  - $eD_k$  : 0 mm
  - $e_x$  : 0 mm
  - $\varphi_{align}$  : 500 mrad
  - $opl_k$  : 500 mm
- Both of them
  - $eD_k$  : 100 mm
  - $e_x$  : 20 mm
  - $\varphi_{align}$  : 500 mrad
  - $opl_k$  : 500 mm

The mean residual of the bar mirror profile is shown as Fig. 16. The results show that the systematic error on the parameter setting 1, 2, and 3 is 4 nm, 3 nm and 7 nm respectively.

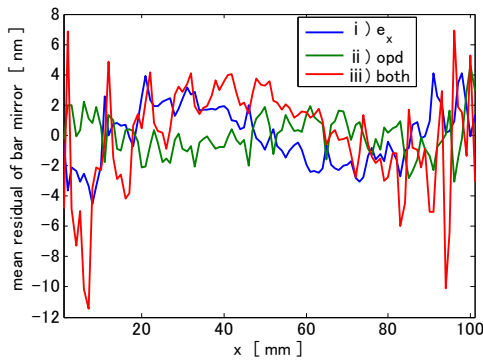


Fig. 16 The effect of non linear terms

**6.3 Effect of the jacobian matrix**

We performed the simulations to evaluate the effect of the jacobian matrix difference. At first, we constructed the  $Y^{nl}$  from the parameters. Then we reconstructed the  $X^{nl}$  from  $Y$  and  $A^{nl}$ . At last, we compared the 10000 times results mean of the reconstructed  $X^{nl}$  with the original  $X$ . The non linear parameters were same as that of 6.2(3). Because the results of  $X$  were unique for each non linear parameter settings, the results wouldn't consequently average.

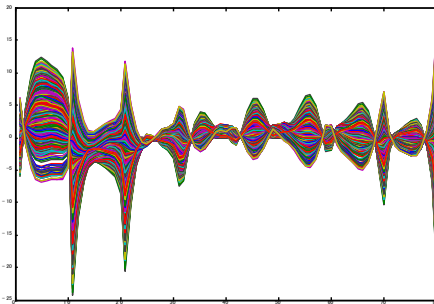


Fig. 17 The residual of the straightness error

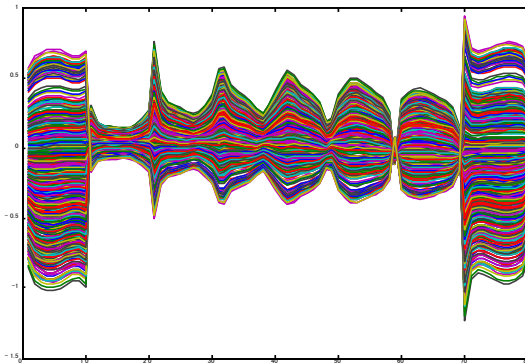


Fig. 18 The residual of the yaw error

**7. Conclusion**

To calibrate the motion error of the M-CMM, we devised a multi-probe method. At first, we used one autocollimator and three laser interferometers to measure the yaw and straightness errors of the stage, and the profile of the bar mirror could be calculated simultaneously, then compared the results of a pre-experiment with that of a white light interferometer. Secondly, we discussed about non linear parameters for estimating the systematic error. At last, we perform a simulation with non linear parameters. The conclusions of this study are summarized as follows:

1. The pre-experiment results showed that the uncertainty with no filter was 11 nm and that with MA filter was 6 nm, which was enough small to calibrate. The mirror profile measuring with a white light interferometer was equal to the pre-experiment result with MA filter.

2. The difference between the mirror profile with MA filter and with no filter was 25 nm and showed the repeatability. This means that the systematic error can't be ignored.
3. The simulation with non linear measuring vector results showed that the average residual of mirror profile between original and reconstructed was 7 nm (Table 4).
4. The simulation with non linear jacobian matrix results showed that the average residual of mirror profile between original and reconstructed was 10 nm (Table 4). In the real measurement, this effect as one set of differences, not as a average of that.

The estimation and simulation result shows that yaw error affects systematic error, while random error consists mainly of laser interferometers' error. To improve the yaw error of moving stage will decrease the systematic error. Our future work is to apply the M-CMM air bearing stage for achieving 2 nm systematic error and 6 nm random error, which is smaller than 10 nm.

The result of pre-experiment	25 nm
From the positioning uncertainty	4 nm
From the optical path difference	3 nm
From the jacobian matrix	10 nm
Total of the non linear terms effects	17 nm

Table 4 The systematic error estimation

**ACKNOWLEDGEMENT**

The present work was supported in part through the Global COE Program, "Global Center of Excellence for Mechanical Systems Innovation," by the Ministry of Education, Culture, Sport, Science and Technology.

**REFERENCES**

- [1] Cao S, Brand U, Kleine-Besten T, Hoffmann W H, Schwenke, B'utefisch S, and B'uttgenbach S. Recent developments in dimensional metrology for microsystem components. *Microsyst. Technol.* 2002;8; 3-6
- [2] Vermeulen MMPA, Rosielle PCJN, and Schellekens PHJ. Design of a high-precision 3D-coordinate measuring machine. *Annals of the CIRP*1998; 47 (1); 447-450
- [3] Mitutoyo, UMAP Vision System, Bulletin No. 1631.
- [4] Bryan JP. The Abbe principle revisited: an updated interpretation. *Prec. Eng.* 1979; 1; 129-32
- [5] Whitehouse DJ. Some theoretical aspects of error separation techniques in surface metrology. *J. of Phys. E: Sci. Instrum.* 1976; 9; 531-536
- [6] Gao W, Yokoyama J, Kojima H, and Kiyono S. Precision measurement of cylinder straightness using a scanning multi-probe system. *Prec. Eng.* 2002; 26; 279-88
- [7] Yang P, Shibata S, Takahashi S, Takamasu K, Sato O, Osawa S, and Takatsuji T. Development of high precision Coordinate Measuring Machine (CMM) (1st report, Evaluation method of XY stage). *JSPE autumn conference 2009*, pp. 725-726
- [8] Yang P, Shibata S, Takahashi S, Takamasu K, Sato O, Osawa S, and Takatsuji T. Development of high precision Coordinate Measuring Machine (CMM) (2nd report, Pre-experiment of multi-probe method for evaluating the XY stage). *JSPE spring conference 2010*, pp. 377-378
- [9] Tomohiko Takamura, Ping Yang, Satoru Takahashi, Kiyoshi Takamasu, Osamu Sato, Sonko Osawa, Toshiyuki Takatsuji, 2010, Development of high precision Coordinate Measuring Machine (CMM) (3rd report, Evaluation of the form of referential mirror and the kinematic error of stage by 3-probe method), 2010 JSPE autumn conference, pp.515-516